Supporting Information

Optical sensing and switching in the visible light spectrum based on the bound states in the continuum formed in GaP metasurfaces

Zhaotang Li[1], Mingcheng Panmai[1], Lidan Zhou[1,2], Shulei Li[1,3], Shimei Liu[1], Jianhua Zeng[4], and Sheng Lan[1,*]

[1] *Guangdong Provincial Key Laboratory of Nanophotonic Functional Materials and Devices, School of Information and Optoelectronic Science and Engineering, South China Normal University, Guangzhou 510006, P. R. China;*

[2] *State Key Laboratory of Optoelectronic Materials and Technologies, School of Electronics and Information Technology, Sun Yat-sen University, Guangzhou 51006, China.*

[3] *School of Optoelectronic Engineering, Guangdong Polytechnic Normal University, Guangzhou 510665, China.*

[4]*School of Physics and Electronic Information, Shangrao Normal University, Shangrao 334001, China*

[*] Correspondence: slan@scnu.edu.cn (S. Lan)

Supplementary Note 1

In Fig. S1, we show the radiation of the GaP "molecule" excited by using a MD source oriented along the *x* direction (i.e., MD_x). The MD source is placed at the center of the GaP "molecule". It can be seen that TD_y and MQ_{xz} can be effectively activated by using MD_x, indicating clearly the interaction between them.

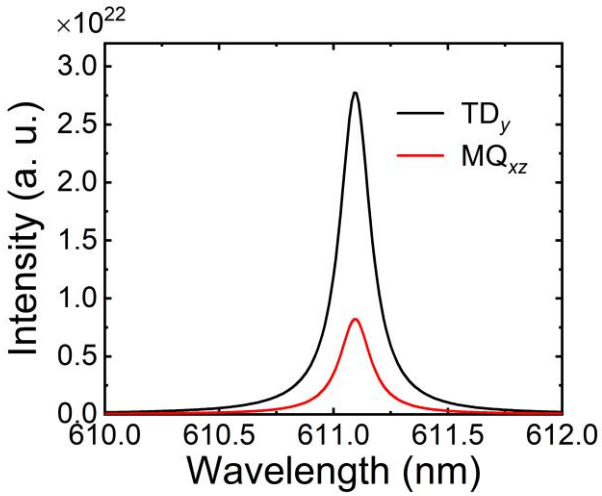

Fig. S1. Radiation from a GaP "molecule" excited by using a MD_x source placed at the center of the GaP "molecule".

Supplementary Note 2

In Fig. S2, we show the ratio of the intensity of MD_x to that of TD_y (i.e., MD_x/TD_y) calculated for metasurfaces with different gap widths (g value). The ratio of the intensity of MQ_{xz} to that of TD_y (i.e., MQ_{xz}/TD_y) is also provided for comparison. It can be seen that MD_x/TD_y decreases exponentially when the gap width (g) approaches g = 45 nm. At g = 45 nm, a minimum value as small as 10^{-6} is observed. In this case, the leakage originating from the interference between MD_x and TD_y/MQ_{xz} is negligible and a maximum Q factor is achieved. In contrast, it is noticed that MQ_{xz}/TD_y remains a constant when g is varied.

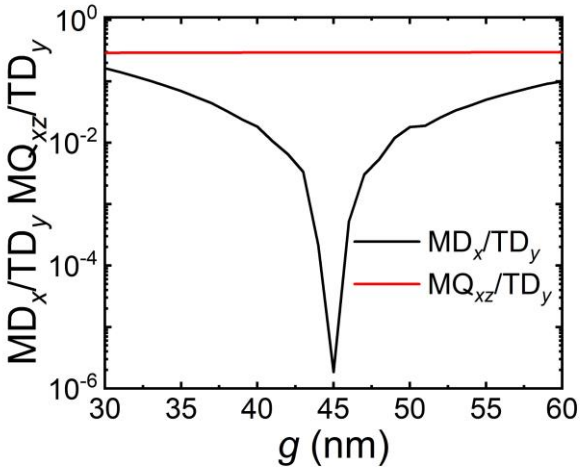

Fig. S2. Dependences of MD_x/TD_y and MQ_{xz}/TD_y on the gap width calculated for the metasurface shown in Fig. 2c.

Supplementary Note 3

We also investigated the influences of the Q factor of the quasi-BIC on the period of the lattice (p) and the width of the GaP cuboid (w), as shown in Fig. S3. In these cases, the gap width (g) between the GaP cuboids was fixed at g = 45 nm. The other structural parameters are the same as those used in Figure 1 in the main text. In Fig. S3a, we show the transmission spectra calculated for the metasurfaces with different periods. One can see a narrowing of the quasi-BIC when p is increased from 290 to 310 nm and a broadening of the quasi-BIC when p is further increased from 310 to 330 nm. The transmission peak disappears at p = 310 nm. In Fig. S3b, we present the dependence of the resonant wavelength and the Q factor of the quasi-BIC on the period of the metasurface (p). A maximum Q factor is observed at p = 310 nm. The Q factor decreases exponentially when p deviates from this value. This behavior is quite similar to that observed in Figure 2b where g is varied. In this case, it is found that the gap width between the neighboring GaP cuboids is equal (g = 45 nm). In Fig. S3b, it is also noted that the resonant wavelength of the quasi-BIC is not sensitive to the change of the period. In Fig. S3c, we show the transmission spectra calculated for metasurfaces composed of GaP cuboids with different widths (w value). Similarly, one can see a narrowing of the quasi-BIC when w is increased from 100 to 110 nm and a broadening of the quasi-BIC when w is further increased from 110 to 120 nm. The transmission peak disappears at w = 110 nm. In Fig. S3d, we present the dependence of the resonant wavelength and the Q factor of the quasi-BIC on the width of the GaP cuboid (w). A maximum Q factor is observed at w = 110 nm. The Q factor decreases exponentially when w deviates from this value. This behavior is quite similar to that observed in Fig. 2b where g is varied. In this case, it is found that the gap width between the neighboring GaP cuboids is equal (g = 45 nm). Differently, a redshift of the quasi-BIC is observed when w is increased. A linear relationship is observed between the resonant wavelength of the quasi-BIC and the width (w).

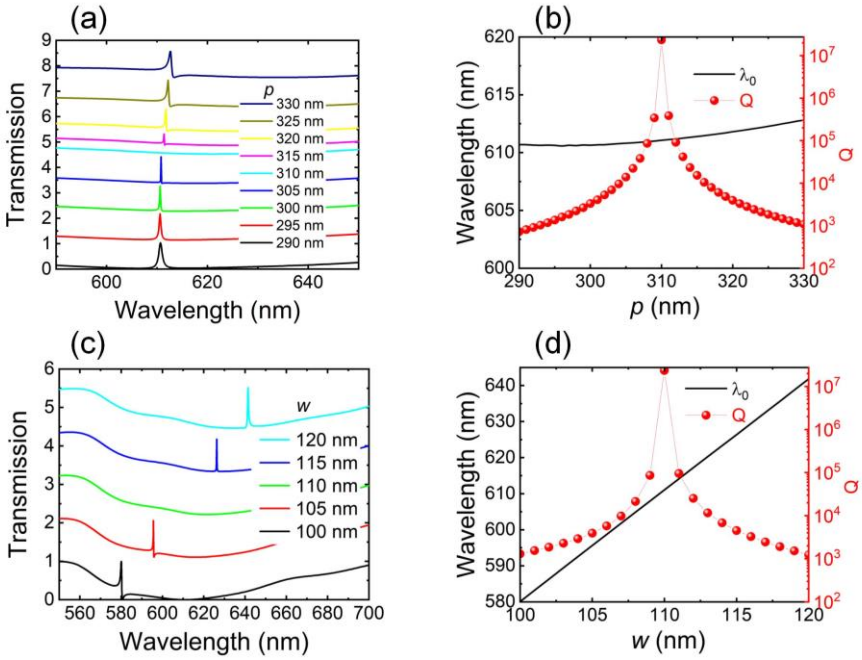

Fig. S3. (a) Transmission spectra calculated for the metasurfaces with different periods. (b) Dependence of the resonant wavelength and Q factor on the period of the metasurface. (c) Transmission spectra calculated for the metasurfaces composed of GaP cuboids with different widths. (d) Dependence of the resonant wavelength and Q factor on the width of the GaP cuboid.

Supplementary Note 4

In Fig. S4, we show the radiation of the GaP "molecule" excited by using an ED source oriented along the *x* direction (i.e., ED_x). The ED source is placed at the center of the GaP "molecule". It can be seen that MD_y and EQ_{xz} can be effectively activated by using ED_x, indicating clearly the interaction between them.

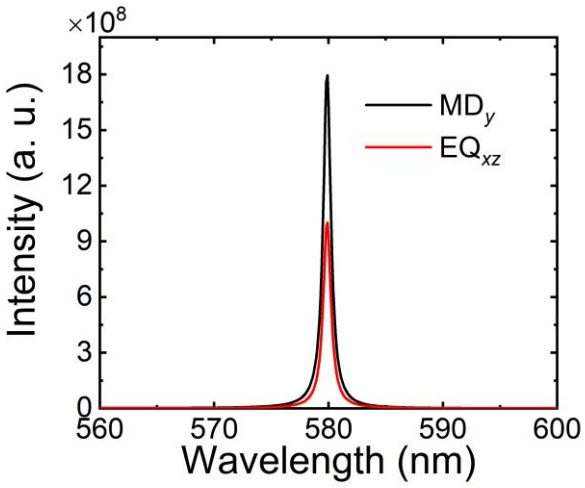

Fig. S4. Radiation from a GaP "molecule" excited by using a ED_x source placed at the center of the GaP "molecule".

Supplementary Note 5

In Fig. S5, we show the ratio of the intensity of ED_x to that of MD_y (i.e., ED_x/MD_y) calculated for metasurfaces with different gap widths (g value). The ratio of the intensity of EQ_{xz} to that of MD_y (i.e., EQ_{xz}/MD_y) is also provided for comparison. It can be seen that ED_x/MD_y decreases exponentially when the gap width (g) approaches g = 45 nm. At g = 45 nm, a minimum value as small as 10^{-5} is observed. In this case, the leakage originating from the interference between ED_x and MD_y/EQ_{xz} is negligible and a maximum Q factor is achieved. In contrast, it is noticed that EQ_{xz}/MD_y nearly remains a constant when g is varied.

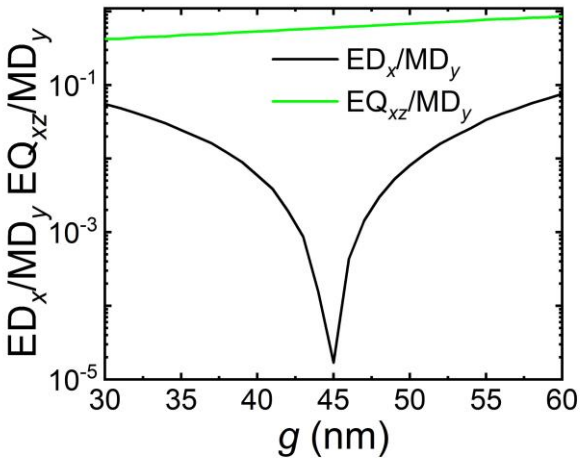

Fig. S5. Dependences of ED_x/MD_y and EQ_{xz}/MD_y on the gap width calculated for the metasurface shown in Fig. 4d.

Supplementary Note 6

In Fig. S6a, we present the radiation patterns of MD_y and EQ_{xz}. The radiation pattern of MD_y appears as a doughnut while that of EQ_{xz} appears as a flower lobe. The interference of MD_y and EQ_{xz} leads to the cancellation of the radiation in the z direction and the enhancement of the radiation in the x direction. Consequently, an 8-shaped radiation pattern is obtained. The coupling between the neighboring unit cells results in a surface wave propagating in the metasurface, as shown in Fig. S6b. If g is chosen appropriately, the radiation loss of the surface wave is quite small, leading to an extremely large Q factor.

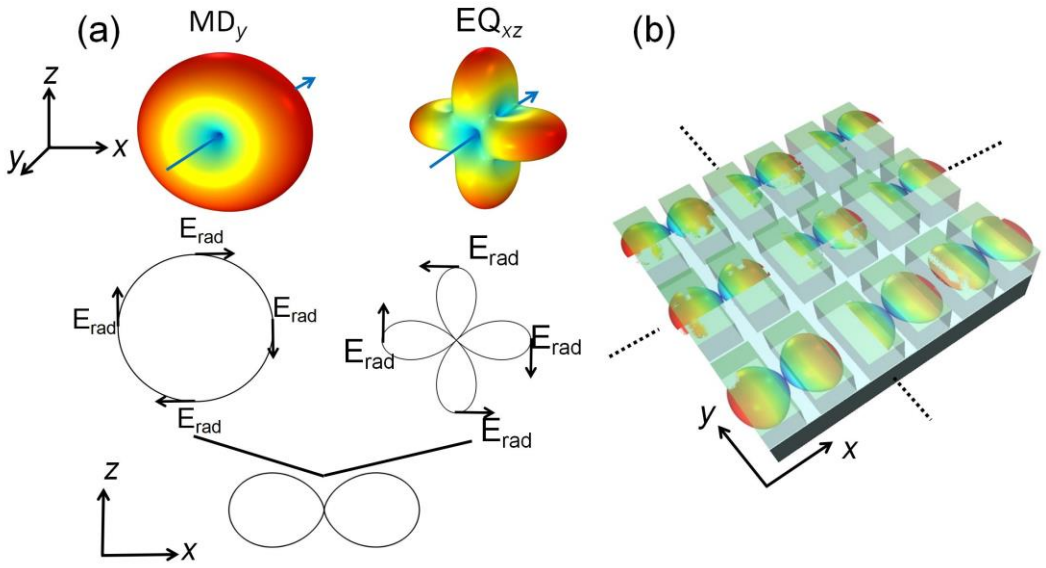

Fig. S6. (a) Three-dimensional radiation patterns of MD_y and EQ_{xz} (upper panel), two-dimensional radiation patterns of MD_y and EQ_{xz} in the XZ plane (middle panel), and the two-dimensional radiation pattern resulting from the interference between MD_y and EQ_{xz} patterns (lower panel). (b) Schematic showing the 8-shaped radiation of the GaP "molecule" and the surface wave formed by the coupling between the radiations of GaP "molecules".

Supplementary Note 7

In Fig. S7a, we show the dependence of the resonant wavelength of the quasi-BIC on the refractive index of the surround environment calculated for metasurfaces with different gap widths (g) excited by x-polarized white light. The results obtained for y-polarized white light are shown in Fig. S7b. In both cases, a linear relationship is observed. The sensitivities extracted from the linear fitting are 135 nm/RIU and 45 nm/RIU, respectively.

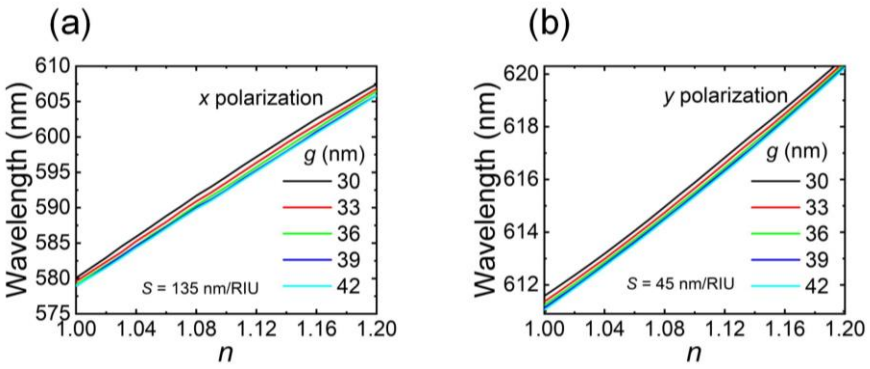

Fig. S7. Dependence of the resonant wavelength of the quasi-BIC on the refractive index of the surround environment calculated for metasurfaces with different gap widths (g) excited by (a) x- and (b) y-polarized white light.